

Accepted Article

Title: Imidazole-Bridged Tetrameric Group(IV) Heteroleptic Complexes from the Spontaneous Metal-Ligand Assembly of a Potentially N4-Tetradentate Ligand

Authors: Lapo Luconi, Giulia Tuci, Dmitry Yakhvarov, Giovanni Poli, Andrea Rossin, Aliya Khusnuriyalova, and Giuliano Giambastiani

This manuscript has been accepted after peer review and appears as an Accepted Article online prior to editing, proofing, and formal publication of the final Version of Record (VoR). This work is currently citable by using the Digital Object Identifier (DOI) given below. The VoR will be published online in Early View as soon as possible and may be different to this Accepted Article as a result of editing. Readers should obtain the VoR from the journal website shown below when it is published to ensure accuracy of information. The authors are responsible for the content of this Accepted Article.

To be cited as: *Eur. J. Inorg. Chem.* 10.1002/ejic.201900763

Link to VoR: <http://dx.doi.org/10.1002/ejic.201900763>

Imidazole-Bridged Tetrameric Group(IV) Heteroleptic Complexes from the Spontaneous Metal-Ligand Assembly of a Potentially N_4 -Tetradentate Ligand

Lapo Luconi,^[a] Giulia Tuci,^[a] Dmitry Yakhvarov,^[b,c] Giovanni Poli,^[d] Andrea Rossin,*^[a]

Aliya Khusnuriyalova^[b,c] and Giuliano Giambastiani *^[a,c,e]

- ^[a] Dr. Lapo Luconi, Dr. Giulia Tuci, Dr. Andrea Rossin, Dr. Giuliano Giambastiani, *Istituto di Chimica dei Composti Organometallici (ICCOM - CNR), Via Madonna del Piano 10, 50019, Sesto Fiorentino, (Italy). Fax: +39 055 5225203. E-mail: giuliano.giambastiani@iccom.cnr.it; a.rossin@iccom.cnr.it. URLs: <http://www.iccom.cnr.it/giambastiani/> (Giuliano Giambastiani); https://www.researchgate.net/profile/Andrea_Rossin (Andrea Rossin)*
- ^[b] Prof. Dmitry Yakhvarov, Ms. Aliya Khusnuriyalova, *Arbuzov Institute of Organic and Physical Chemistry, FRC Kazan Scientific Center of RAS, 420088 Kazan, Russian Federation.*
- ^[c] Prof. Dmitry Yakhvarov, Ms. Aliya Khusnuriyalova, *Kazan Federal University, 420008 Kazan, Russian Federation*
- ^[d] Prof. Giovanni Poli, *Sorbonne Université, Faculté des Sciences et Ingénierie, CNRS, Institut Parisien de Chimie Moléculaire, IPCM, 4 place Jussieu, 75005 Paris, France*
- ^[e] Dr. Giuliano Giambastiani, *Institut de Chimie et Procédés pour l'Energie, l'Environnement et la Santé (ICPEES), UMR 7515 CNRS- University of Strasbourg (UdS), 25, rue Becquerel, 67087 Strasbourg Cedex 02, France. E-mail: giambastiani@unistra.fr URL : <https://www.trainermopga.com/>*

Abstract. The imidazole-containing N_4 -tetradentate ligand N-(2-(1H-imidazol-2-yl)-3-(pyridin-2-yl)propyl)-2,6-diisopropylaniline ($L2^H$) and its N-benzyl-protected variant ($L2^{Bn}$) at the imidazole fragment have been synthesized and fully characterized. Both molecules contain an unresolved C_{sp^3} stereogenic center. The coordination behavior of the newly prepared ligands towards Group IV metal ions ($M^{IV} = Zr, Hf$) has been examined through multinuclear 1H and $^{13}C\{^1H\}$ NMR spectroscopy and selected single crystal X-ray structural analyses. The ability of the imidazole fragment to enter the metal coordination sphere as a neutral or a monoanionic system has been also investigated, unveiling quite original coordination modes as well as unexpected molecular architectures. When one N imidazole atom

is blocked by a benzyl protecting group ($\mathbf{L2}^{\text{Bn}}$), the ligand reaction with $\text{M}^{\text{IV}}(\text{NMe}_2)_4$ ($\text{M}^{\text{IV}} = \text{Zr, Hf}$) as metal precursor gives rise to discrete monometallic tris(dimethylamido) 5-coordinated compounds of general formula $\mathbf{L2}^{\text{Bn}}\text{M}(\text{NMe}_2)_3$. The ligand chelates the metal ion as a bidentate monoanionic $\kappa^2\{\text{N}^-, \text{N}\}$ system through the imidazole moiety and the anilido N donor while an uncoordinated picolyl arm dangles away from the metal center. Upon coordination to the metal ion, the unprotected $\mathbf{L2}^{\text{H}}$ undergoes a unique self-assembly of the chiral racemic ligand to generate an achiral tetrameric network featuring a regularly alternating (R^*, S^*, R^*, S^*) configuration around the 6-coordinated metal centers. The resulting bis(dimethylamido) tetrameric architectures of formula $[\mathbf{L2}^{\text{H}}\text{M}(\text{NMe}_2)_2]_4$ named “poker complexes” contain the imidazole fragment of each ligand bridging two adjacent M^{IV} ions in a $\mu\text{-}\kappa\{\text{N}^-\}:\kappa\{\text{N}^-\}$ coordination hapticity. At the same time, the picolyl fragments of each chelating $\mathbf{L2}^{\text{H}}$ ligand “sting” a neighboring metal center as unconventional scorpion’s tails that impose further rigidity to the tetrameric structure.

Keywords. Zirconium(IV) – Hafnium(IV) – imidazole – supramolecular assembly – N-ligands

Introduction

The design and synthesis of organic ligands featured by tunable donor atom sets represent a steadily growing research area still attracting the interest of the worldwide coordination chemistry and homogeneous catalysis audience. To this aim, significant efforts have been devoted to tailor electronic and steric ligands properties and to accommodate various metal ions in their binding pockets as to get organometallics or coordination compounds featured by targeted catalytic requirements.^[1] In particular, the preparation of multidentate N-ligands ($\text{N} > 2$) and the study of their metal ion coordination behavior is a well-developed research area in contemporary organometallic chemistry.^[2-13] The introduction of aromatic N-containing heterocycles like pyridine,^[14] triazole^[15] or pyrazole^[16-17] has contributed to

expand the variety of N-multidentate backbones. Their hapticity varies as a function of the degree of the ligand's skeleton flexibility. A classical structural scheme for a tridentate ligand is given by a central donor atom flanked by two "side-arms" containing other coordinative moieties. For these ligands, five-coordinated or six-coordinated species are commonly obtained. Depending on the ligand flexibility, they may adopt either a "mer" or a "fac" arrangement of their donor atoms (Figure 1).

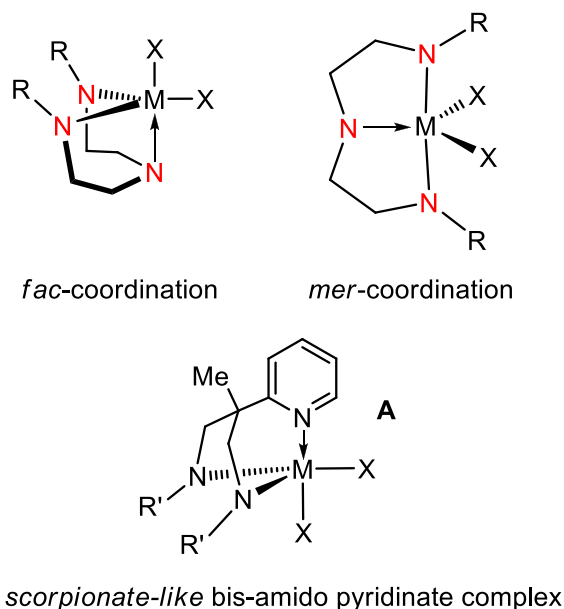
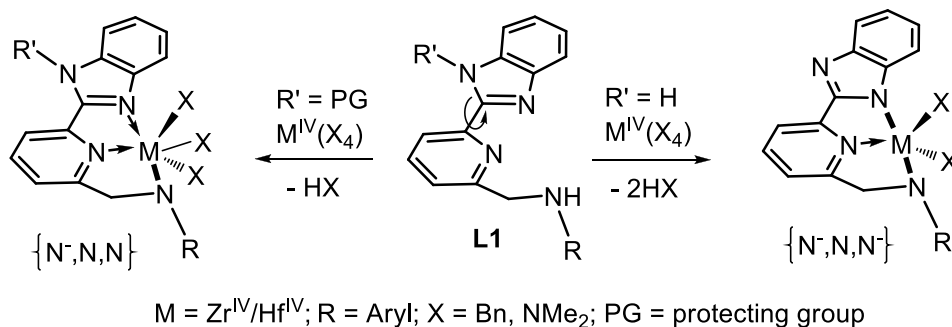


Figure 1. *fac* vs. *mer* coordination mode in a tridentate N-containing ligand adopting a five-coordinate geometry. Coordination compounds **A** (with variable R' groups) are a seminal example of complexes bearing a tripodal *fac*-coordinated ligand from the literature (see ref. [18]).

An important exception to this general scheme is given by the bis-amido pyridinate ligand **A** (Figure 1) presented by Gade and co-workers in 1997.^[18] Like the pincer of a scorpion, this versatile class of ligands binds the metal center with two nitrogen atoms from two amidate groups on the equatorial positions while a third N-site from the pyridinic fragment linked to a Csp³ atom "stings" the metal ion like a scorpion's tail. Thus, the coordination geometry is restricted to *fac*. At the same time, the T-shaped *mer* coordination mode is precluded if the pyridine donor atom is bound to the metal ion. Since their discovery, these tripodal systems have been widely investigated with respect to their arrangement in the

coordination sphere of highly electrophilic tetravalent metal ions^[19] as well as for the inherent catalytic properties^[20-25] of the resulting coordination compounds.

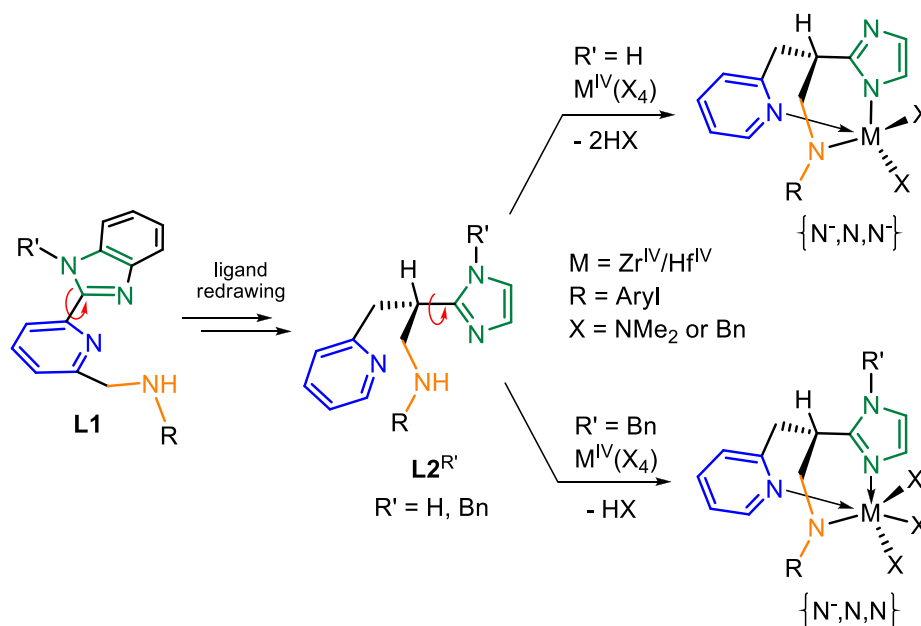
In recent years, our group has been extensively working on the preparation of multidentate heteroleptic N-ligands and their related $\kappa^3\{\text{N,N,N}\}\text{M}^{3+/4+}$ coordination compounds (or $\kappa^3\{\text{N,C,N}\}\text{M}^{3+/4+}/\kappa^3\{\text{N,N,C}\}\text{M}^{3+/4+}$ organometallics) based on highly electrophilic metal ions (from Group IV elements of the periodic table^[26-32] or from lanthanides^[31, 33-37]) for applications in homogeneous catalysis. In a recent report, we have described the synthesis, characterization and catalytic application of a series of $\text{Zr}^{\text{IV}}/\text{Hf}^{\text{IV}}$ alkyl/amido complexes stabilized by a tridentate N-ligand containing a benzoimidazole fragment.^[32] We have shown the ability of this ligand system to vary its coordination mode around the metal ion and thus the ultimate complex coordination number by means of a protection/deprotection switch of the pyrrolic N-site at the “rolling” imidazole pendant arm (Scheme 1).



Scheme 1. Tunable $\kappa^3\{\text{N,N,N}\}\text{L1}$ ligand pocket by NH protection/deprotection of a rolling benzoimidazole pendant arm and its coordination to $\text{Zr}^{\text{IV}}/\text{Hf}^{\text{IV}}$.^[32]

Imidazole (and its derivatives) is one of the most intriguing^[38] and stable N-heterocycles to be employed in coordination chemistry. Due to the ability of its deprotonated form (imidazolate) to act as a bridging ligand with a wide variety of metal ions, it has already provided a number of polymetallic materials and original complex architectures.^[39] Starting from our interest in the synthesis and characterization of Group IV pyridylamido complexes containing pyrazole^[28-29] and imidazolate^[32] units, we report herein

on the synthesis and coordination chemistry of a new imidazolate-based polydentate N-ligand. Our aim was to redistribute the spatial assembly of the donor atom set in **L1** to create a new molecular architecture **L2** to be employed as tridentate mono- or di-anionic $\kappa^3\{N,N,N\}$ system for Group IV metal ions coordination (Scheme 2). The idea was to move towards a “scorpionate-like” system, closely related to the celebrated bis-amido pyridinate ligand **A** (Figure 1), whose versatility in coordination chemistry and catalysis is well-known.^[19-25] The coordination behavior of the newly prepared ligand towards Zr^{IV} and Hf^{IV} has been investigated, playing on the ability of imidazole to enter the metal coordination sphere as a neutral or a monoanionic system.



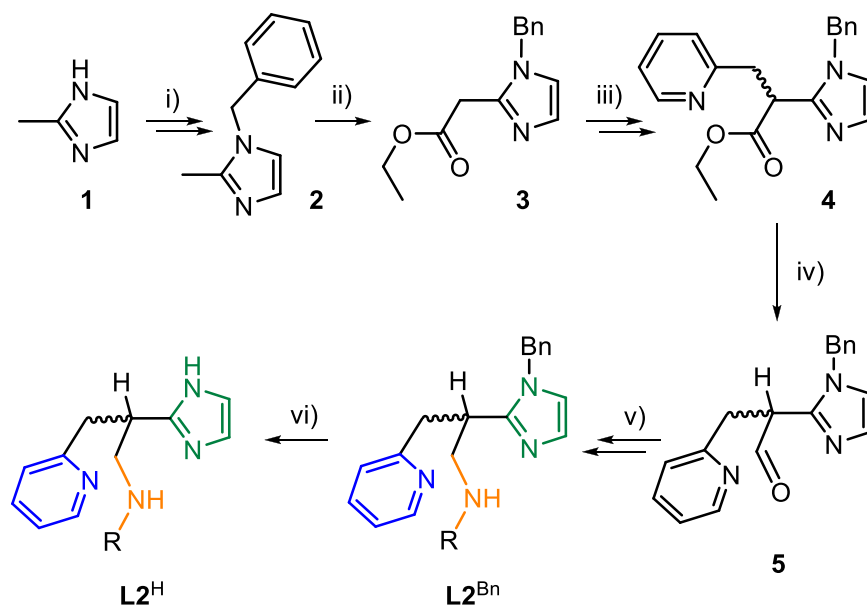
Scheme 2. Redrawing the donor atom set of **L1** into a new **L2** architecture featured by a “scorpionate-like” spatial arrangement of the N-coordinating groups and an electronically tunable ligand pocket.

To this aim, a radically different synthetic protocol from that previously described for **L1** has been established and the ligand reactivity with classical Group-IV tetra(amido) metal precursors [$M^{IV}(NMe_2)_4$, $M^{IV} = Zr^{IV}$ or Hf^{IV}] has been investigated. At odds with the postulated metal-ligand reactivity, an

unexpected tendency of the $L2^{R'}$ deprotected system ($R' = H$) to undergo spontaneous self-assembly into original and multinuclear coordination compounds has been observed.

Results and Discussion

Synthesis of amido-pyridinate $L2^{R'}$ ligands ($R' = L2^H$ or $L2^{Bn}$) containing the N-H free or the N-Bn protected imidazole unit. Scheme 3 illustrates the stepwise procedure to the preparation of the chiral scorpionate-type $L2^H$ and $L2^{Bn}$ ligands. Both systems share the same synthetic path, with the exception of the last Pd-catalyzed hydrogenation step used for the benzyl removal from the imidazole fragment of $L2^{Bn}$ to get $L2^H$.



Scheme 3. Synthesis of $L2^{R'}$ ligands. Reagents and conditions: i) NaH, 273 K; benzyl-bromide, THF, reflux, 1h, isolated yield: > 99 % ii) ClCOOEt, Et_3N , CH_3CN , r.t. 2h, isolated yield: 57 %. iii) 1) NaH, 273 K; 2-(chloromethyl)pyridine, DMF, r.t., 2 h, isolated yield: 63 %. iv) DIBAL-H, CH_2Cl_2 , 195 K, isolated yield: 78 %. v) 2,6- $iPr(C_6H_3)NH_2$, neat, 273 K, overnight; $NaBH_3CN$, AcOH, THF/MeOH, 323 K, 3h, isolated yield: 75 %. vi) $Pd(OH)_2/C$, MeOH, 323 K, H_2 (3 bar), 20h, isolated yield: 45 %.

Although a certain degree of improvement in each synthetic step remains possible (at least in terms of isolated yields), the synthetic efforts devoted to the new ligands design and synthesis may be useful for

the development of future molecular architectures. Therefore, we provide a concise description of each synthetic step before discussing the ligands coordination chemistry towards Group-IV metals. According to Scheme 3, **L2^{Bn}** and **L2^H** were obtained through five and six synthetic steps as analytically pure compounds in the form of a pale yellow oil (**L2^{Bn}**) and white crystals (**L2^H**), respectively (see Experimental section). The ligands synthesis starts with the protection of the commercially available 2-methyl-1*H*-imidazole (**1**) with a benzyl group to prevent undesired side-reactions at the heterocycle core throughout the multi-step synthetic path. Hence, the reaction with benzylbromide (BnBr)^[40] was carried out to generate the 1-benzyl-2-methyl imidazole (**2**). Treatment of **2** with ethyl chloroformate^[40-41] gave **3** as a pale yellow oil in 57 % isolated yield over two steps. The introduction of the pyridine pendant fragment was accomplished by deprotonation of the acidic methylene fragment of **3** followed by nucleophilic substitution on a freshly prepared 2-picolyl chloride solution.^[42] The latter was released from the hydrochloride adduct^[43] upon salt washing with an aqueous NaHCO₃ solution (pH = 8) followed by extraction in organic solvents.^[44] The HCl-free 2-picolyl chloride was used immediately in the nucleophilic substitution with **3**⁻Na⁺ without any further purification. The reaction afforded the ethyl ester **4** that was recovered after chromatographic purification in the form of yellow crystals in 63 % yield. The isolated intermediate was then reduced to aldehyde **5** through treatment with DIBAL-H under controlled conditions. **5** was used in turn for the *one-pot* reductive amination^[45-47] reaction with 2,6-*i*Pr(C₆H₃)NH₂, followed by *in-situ* treatment with a NaBH₃CN/AcOH mixture to give **L2^{Bn}** as a viscous yellow pail oil after chromatographic purification. Finally, various conditions were scrutinized to carry out the **L2^{Bn}** debenzilation step by reductive cleavage of the protecting group over palladium metal catalysts.^[48-50] Among the various heterogeneous systems tested, Pearlman's conditions^[51-52] [Pd(OH)₂/C in hot MeOH (323 K)]^[53] were the most effective to obtain **L2^H** in fairly good yield after catalyst filtration and chromatographic purification of the crude mixtures.

With the synthetic procedure for the new amido-pyridinate ligands in hands, we started to study their reactivity upon coordination/transamination reactions on model and highly reactive Group-IV metal tetrakis(dimethylamido) precursors of general formula $M(\text{NMe}_2)_4$. The study has unveiled unexpected reactivity paths leading to the isolation of original coordinative architectures that are (in some cases) rather far from our expectations.

Reactivity and coordination behavior of $\mathbf{L2^{Bn}}$ and $\mathbf{L2^H}$ with $\text{Zr}^{\text{IV}}(\text{NMe}_2)_4$ and $\text{Hf}^{\text{IV}}(\text{NMe}_2)_4$. Neutral tris(amido) Zr^{IV} and Hf^{IV} compounds of general formula $[\mathbf{L2^{Bn}}M(\text{NMe}_2)_3]$ ($M=\text{Zr}^{\text{IV}}, \text{Hf}^{\text{IV}}$) were straightforwardly obtained upon mixing an equimolar amount of a tetravalent metal precursor $[\text{Zr}(\text{NMe}_2)_4$ or $\text{Hf}(\text{NMe}_2)_4]$ with $\mathbf{L2^{Bn}}$. The reaction was initially accomplished in a J-Young NMR tube as to follow its course spectroscopically. ^1H NMR spectra of both solutions revealed that reactions proceeded smoothly in benzene- d_6 already at room temperature to give solutions containing unique coordination compounds $[\mathbf{L2^{Bn}}\text{Zr}(\text{NMe}_2)_3]$ (**6**) and $[\mathbf{L2^{Bn}}\text{Hf}(\text{NMe}_2)_3]$ (**7**, Figure 2), respectively], as tris(dimethylamido) forms. With both metal precursors, the ligand complexation was extremely clean and complete within 30 min. For the sake of completeness, the reaction mixtures were kept at room temperature overnight and then heated at reflux for 3 h. After this prolonged treatment, the reaction mixture was left unchanged and no new coordination compounds were generated. Moreover, no appreciable decomposition of the initially formed species was observed. This fact highlights the favored thermodynamic ligand arrangement around the metal ions as well as the relatively high complexes stability in solution. ^1H and $^{13}\text{C}\{^1\text{H}\}$ NMR patterns of both species showed largely superimposable profiles, with distinct sets of signals for aliphatic and aromatic protons and carbons (Figure S9-S12). The most relevant ^1H NMR spectral features of **6** and **7** are represented by the presence of two well distinct pairs of resonances for the diastereotopic methyl groups of the isopropyl moiety (four doublets at $\delta_{\text{H}} = 1.21/1.57$ and $1.20/1.58$ ppm, respectively). In addition, the diastereotopic methylene protons of the $-\text{CH}_2-$ group bridging the stereogenic center with the anilido groups is a poorly resolved ABX system,

with two sets of signals at $\delta_{\text{H}} = 3.34$ and 4.10 or $\delta_{\text{H}} = 3.60$ and 4.11 ppm for **6** and **7**, respectively. The isopropyl fragments on the $^{13}\text{C}\{^1\text{H}\}$ NMR spectrum of **6** and **7** give rise to six distinct resonances in the $\delta_{\text{C}} = 24.2\text{--}28.8$ ppm range. The singlet attributed to the bridging methylene carbon between the stereogenic center and the anilido moiety is the only $-\text{CH}_2-$ fragment appreciably shifted (≈ 7 ppm) to lower fields with respect to the free-ligand. All these features account for relatively rigid ligands configuration around the metal ions likely due to a chelating action of L2^{Bn} as either a bidentate monoanionic $\kappa^2\{\text{N}^-, \text{N}\}$ or a tridentate monoanionic $\kappa^3\{\text{N}^-, \text{N}, \text{N}\}$ system. Analytically pure crystals of **7** suitable for X-ray analysis were isolated in the form of cubic colorless microcrystals from a concentrated and cooled *n*-pentane solution and a perspective view of its structure is given in Figure 2.

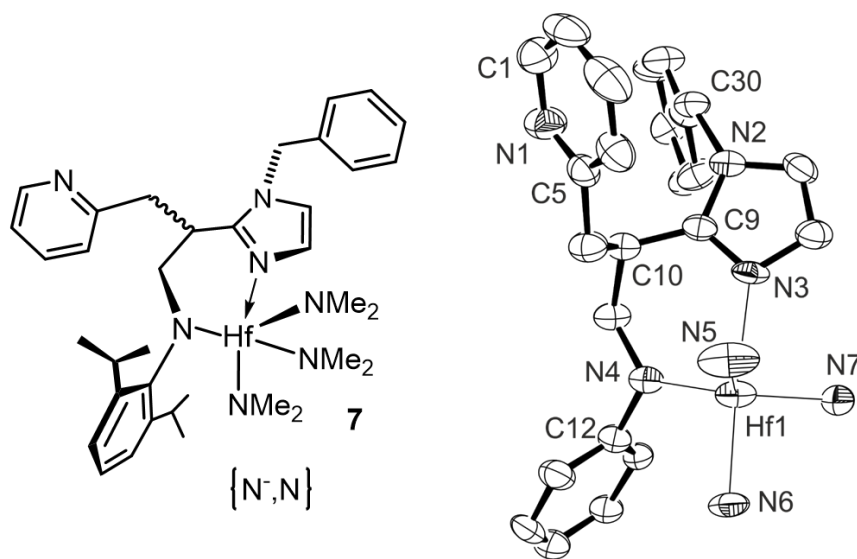


Figure 2. (left) Molecular representation of the $\kappa^2\{\text{N}^-, \text{N}\}$ complex **7** and (right) ORTEP representation of its X-ray structure with ellipsoids shown at 50 % probability. For the ORTEP representation, hydrogen atoms, *i*Pr groups and methyl fragments on the residual $-\text{NMe}_2$ moieties are omitted for clarity. Only the R enantiomer in the asymmetric unit is represented for the sake of simplicity.

Compound **7** crystallizes in the (achiral) triclinic $P\bar{1}$ space group with two molecules in the asymmetric unit (containing R and S enantiomeric ligand forms). Each metal ion maintains a distorted trigonal

bipyramidal coordination geometry (coordination number 5).^[54] At odds with our pristine expectations, **L2^{Bn}** enters the coordination sphere as a bidentate monoanionic $\kappa^2\{N^-,N\}$ system, with the uncoordinated picolyl arm dangling away from the metal center. To the best of our knowledge, this is the first example of a structurally characterized hafnium(IV) imidazole complex to date. The main structural metrics [$\bar{d}(\text{Hf-N}_{\text{im}}) = 2.37 \text{ \AA}$; $\bar{d}(\text{Hf-N}_{\text{anilido}}) = 2.12 \text{ \AA}$; $\bar{d}(\text{Hf-NMe}_2) = 2.08 \text{ \AA}$; $\alpha(\text{N}_{\text{im}}\text{-Hf-N}_{\text{anilido}}) = 79.8^\circ$] fall in the typical range observed for similar complexes in the CSD containing anilido ligands bound to hafnium(IV) [$\bar{d}(\text{Hf-N}_{\text{anilido}}) = 2.11 \text{ \AA}$].^[28-30, 55-59] Intramolecular C-H...N interactions are present in the molecule between C-H bonds from methylene or dimethylamido groups and N-atoms from the same -NMe₂ ligands or from the uncoordinated pyridine [$d(\text{C}\cdots\text{NMe}_2) = 3.662(7) \text{ \AA}$; $d(\text{C}\cdots\text{N}_{\text{py}}) = 3.483(12) \text{ \AA}$]. The main crystal and structural refinement data are listed in Table S1 while selected bond lengths and angles are summarized in Table 1.

When the deprotected **L2^H** ligand was reacted in a 1:1 molar ratio with $\text{M}(\text{NMe}_2)_4$ ($\text{M} = \text{Zr}^{\text{IV}}$ or Hf^{IV}) a fast color change (from colorless to pale yellow) took place almost instantaneously. The reaction course was followed *via* ¹H NMR spectroscopy in a J-Young NMR tube at room temperature and at fixed reaction times. With both metal precursors, the ¹H NMR spectra revealed the generation of complex mixtures of undefined soluble species without any appreciable modification/evolution in the mixture composition even after keeping the solution at room temperature for prolonged times (1 or 2 h). Under these conditions, only few distinctive signals were unambiguously ascribed to selected fragments (*i.e.* dimethylamino groups and isopropyl moieties). Noteworthy, a prolonged heating (7 h) at 343 K of the benzene-*d*₆ mixture containing $\text{Zr}(\text{NMe}_2)_4$ as metal precursor showed a progressive evolution towards a single well-defined form whose identification remained hard to be addressed on the unique basis of the ¹H NMR and ¹³C{¹H} NMR spectra recorded on the crude sample. On the contrary, the same reaction conditions applied to the **L2^H**/ $\text{Hf}(\text{NMe}_2)_4$ mixture did not cause any appreciable modification in the

products composition. Under harsher conditions (toluene-*d*₈, T = 373 K), the **L2^H**/ Hf(NMe₂)₄ mixture underwent an identical evolution of its Zr(NMe₂)₄ counterpart, with formation of one well-defined new species. Reactions with both metal precursors were then scaled-up and carried out in batch while keeping the systems at 343 K in benzene (Zr) and 373 K in toluene (Hf) for seven and fifteen hours, respectively. After that time, both solutions were evaporated to dryness under reduced pressure to obtain crude yellow solids that underwent slow crystallization from hot *n*-pentane. Yellow microcrystals of analytically pure compounds [**8** (Zr); **9** (Hf)] were then isolated in 61% and 58% yield, respectively. The moderate isolated yields obtained were ascribed to the high solubility of both compounds in aromatic and aliphatic solvents. Both complexes were fully characterized in solution, while the solid state structure of **8** was determined through X-ray diffraction. The presence of minor resonances in the ¹H NMR spectrum of both crude mixtures (not belonging to the starting reagents) accounted for the generation of other species whose identification was other than trivial; thus, they were no further processed (see Figure S15). ¹H and ¹³C{¹H} NMR spectra (benzene-*d*₆, 293 K) of both isolated compounds (**8** and **9**) showed largely superimposable regions that accounted for the generation of the same coordination compounds irrespective to the metal precursor used (Figures S13–S14 and S16–S17). ¹H NMR profiles showed set of well-defined signals with chemical shifts and integrals consistent with the formation of bis(amido) adducts. The disappearance of diagnostic NH signals from both the alkyl aniline fragment and the imidazole group in **L2^H** led to the hypothesis that a double transamination reaction took place, with concomitant ligand chelation in its bis(amidate) dianionic form. In addition, the bridging diastereotopic methylene fragment on the pyridine unit gave two well distinct proton resonances (ABX system at δ_H ≈ 2.7/4.6 ppm and 2.8/4.8 ppm for **8** and **9**, respectively) consistent with a rigid conformation of the entire arm, likely due to the participation of the pyridine core to the metal coordination sphere. Finally, the ¹³C{¹H} NMR spectrum confirmed the supposed generation of a new tetra(amidate) zirconium complex; its unique distinctive feature is represented by two singlets attributed to the residual NMe₂ groups (δ_C =

45.3 and 46.2 ppm for **8** and 45.4 and 46.3 ppm for **9**). In order to get additional insight on the ligand coordination hapticity, crystals suitable for X-ray diffraction analysis were grown by successive and slow re-crystallizations of the isolated compounds at room temperature from concentrated hot *n*-pentane solutions. Surprisingly, the X-ray structural analysis of **8** revealed a coordination mode of $L2^H$ more complex than that supposed on the basis of the NMR analysis. The solid state structure of the isolated zirconium compound revealed the generation of an original tetrameric compound with unit formula $L2^HZr(NMe_2)_2$, where each potentially tetradentate ligand chelates two neighboring metal ions in a $\mu\text{-}\kappa^2\{N^-,N^-\}:\kappa^2\{N,N\}$ hapticity. Each metal center in **8** has coordination number 6, made of two residual NMe_2 fragments, two amido groups and two N-pyridine donors from distinct bridging ligand units (Figure 3).

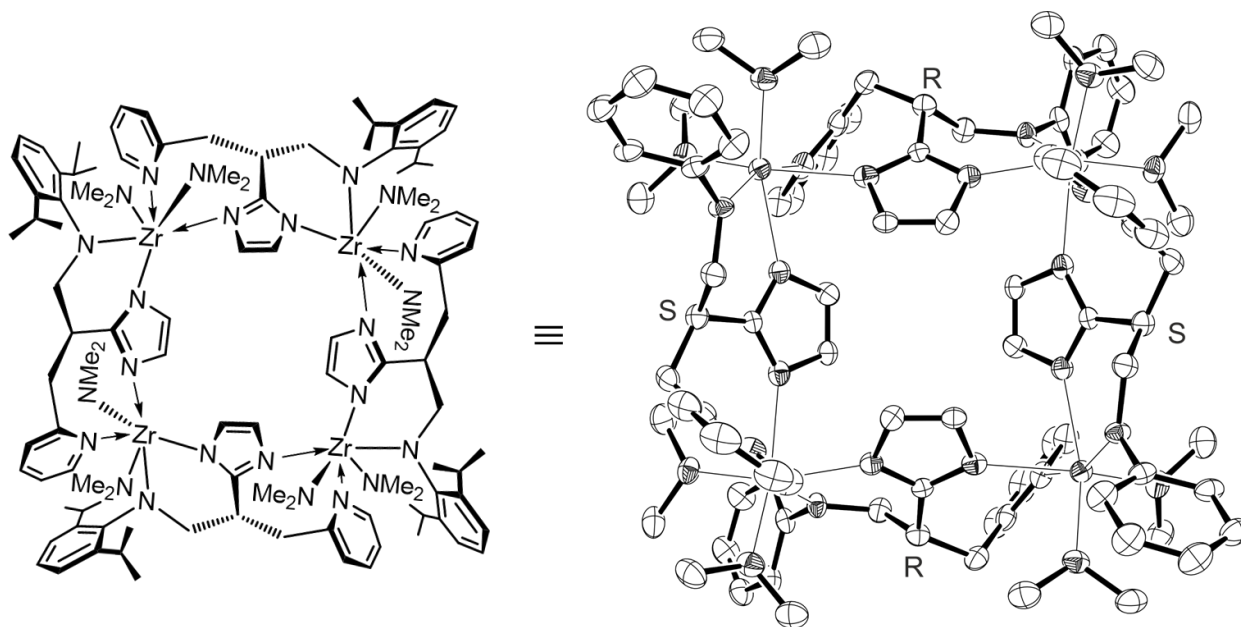


Figure 3. (left) Molecular representation of the $\mu\text{-}\kappa^2\{N^-,N^-\}:\kappa^2\{N,N\}$ tetrameric complex **8** and (right) ORTEP representation of its X-ray structure with ellipsoids shown at 50 % probability. For the ORTEP representation, hydrogen atoms, iPr groups and one molecule of *n*-pentane crystallization solvent are omitted for clarity. Molecular labels are omitted from the ORTEP representation for the sake of clarity. Labels are reported on Figure S18.

Each imidazole ring bridges two neighboring zirconium ions (μ - κ -N: κ -N⁻ coordination hapticity). All metal centers feature a distorted octahedral coordination geometry with an anilido group and a pyridinic moiety from two distinct ligand units occupying the axial positions. Finally, two *cis*-NMe₂ fragments, an amido group and a pyridinic nitrogen from two distinct imidazole frameworks lie on equatorial positions of each octahedron. Compound **8** crystallizes as a *n*-pentane solvate in the (achiral) tetragonal $I\bar{4}$ space group with eight monomers (*i.e.* two full tetramers) in the unit cell. The asymmetric unit contains only one Zr atom and one ligand, according to the minimal formula $L_2^H Zr(NMe_2)_2$ reported above. The tetrameric structure is obtained through the application of the symmetry elements of the $I\bar{4}$ space group in the lattice. The main structural metrics [$\bar{d}(Zr-N_{im}) = 2.36 \text{ \AA}$; $d(Zr-N_{py}) = 2.495(4) \text{ \AA}$; $d(Zr-N_{anilido}) = 2.120(4) \text{ \AA}$; $\bar{d}(Zr-NMe_2) = 2.09 \text{ \AA}$; $\alpha(N_{im}-Zr-N_{im}) = 77.22(13)^\circ$; $\alpha(N_{im}-Zr-N_{py}) = 76.55(13)^\circ$; $\alpha(N_{im}-Zr-N_{anilido}) = 80.34(14)^\circ$] fall in the typical range observed for similar complexes in the CSD containing bridging^[39] or terminal^[60-61] imidazole ligands bound to zirconium(IV) [$\bar{d}(Zr-N_{im}) = 2.33 \text{ \AA}$; $\bar{\alpha}(N_{im}-Zr-N_{im}) = 97.3^\circ$; $\bar{\alpha}(N_{im}-Zr-N_{py}) = 74.1^\circ$]. Intramolecular C-H \cdots N interactions are present in the molecule between C-H bonds from methylene or dimethylamido groups and N-atoms from the same -NMe₂ ligands or imidazole [$d(C\cdots NMe_2) = 3.379(6) \text{ \AA}$; $d(C\cdots N_{im}) = 3.214(7) \text{ \AA}$]. The imidazole nitrogen atoms lie slightly out of the Zr₄ plane (mean distance = 0.37 \AA). The main crystal and structural refinement data are listed in Table S1 while selected bond lengths and angles are summarized in Table 1. Notably, each ligand unit in the tetramer is spatially arranged as to generate a regular alternation of the imidazoles pointing the cage center. Similarly, 2-picoline dangling arms alternately lie above and below the Zr₄ plane. Such a molecular architecture is the result of a unique assembly of the chiral racemic ligand into an achiral tetrameric network featuring regularly alternating R/S ligand enantiomers. From a structural analysis of **8**, a C₂ axis passing through the center of the tetrameric architecture and lying perpendicular to the Zr₄ plane can be found as a symmetry element. In addition, an S₄ roto-reflection axis is also present as additional symmetry element, coincident with C₂. As it can be seen from the representation outlined

on Figure 4, the application of the S_4 symmetry operation on **8** (*i.e.* a 90° rotation around a hypothetical C_4 axis followed by a reflection in a mirror plane σ_h perpendicular to it) gives back the same initial structure. Accordingly, such an assembly gives rise to an *achiral* structure of S_4 symmetry.^[62-65] Although the analysis of the crude reaction mixture does not rule out the generation of other chiral or achiral assemblies, the prolonged reaction heating at 343 K of solvent gave **8** as the largely prevalent and thermodynamically favored species, characterized by a high crystallinity degree.

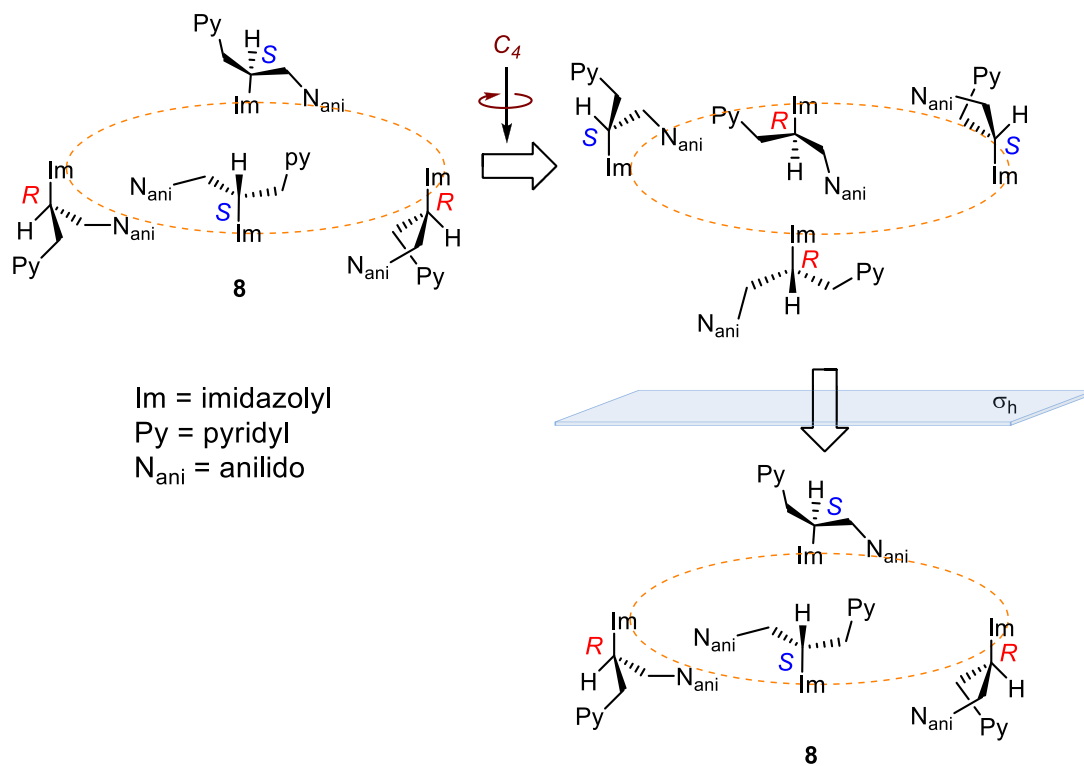


Figure 4. S_4 roto-reflection axis on the achiral structure of **8**. Substituents priorities on the stereogenic centers have been assigned on the basis of the Cahn-Ingold-Prelog rules.

Table 1. Selected bond distances (Å) and angles ($^\circ$) for complexes **7** and **8**.

	7 (M = Hf)	8 (M = Zr)
M(1)-N(1)	-	2.495(4)
M(1)-N(2)	-	2.353(4)

M(1)-N(3)	2.378(4)	2.368(4)
M(1)-N(4)	2.126(4)	2.120(4)
M(1)-N(5)	2.062(5)	2.086(4)
M(1)-N(6)	2.084(4)	2.091(4)
M(1)-N(7)	2.067(5)	-
N(5)-M(1)-N(6)	95.79(18)	97.03(17)
N(5)-M(1)-N(4)	124.10(17)	94.57(16)
N(6)-M(1)-N(4)	99.89(17)	103.70(16)
N(5)-M(1)-N(2)	-	162.45(16)
N(6)-M(1)-N(2)	-	100.48(16)
N(4)-M(1)-N(2)	-	80.34(14)
N(5)-M(1)-N(3)	81.31(17)	87.64(15)
N(6)-M(1)-N(3)	175.90(18)	152.87(15)
N(4)-M(1)-N(3)	79.52(15)	102.53(15)
N(2)-M(1)-N(3)	-	77.22(13)
N(5)-M(1)-N(1)	-	106.35(15)
N(6)-M(1)-N(1)	-	76.49(15)
N(4)-M(1)-N(1)	-	158.95(15)
N(2)-M(1)-N(1)	-	78.96(14)
N(3)-M(1)-N(1)	-	76.55(13)
N(5)-M(1)-N(7)	112.39(18)	-
N(7)-M(1)-N(6)	95.12(19)	-
N(7)-M(1)-N(4)	119.05(18)	-
N(7)-M(1)-N(3)	88.69(17)	-

Conclusions

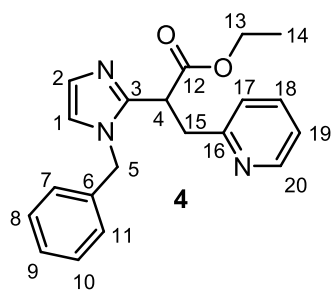
The attempt to move towards new “scorpionate-like” systems based on heteroleptic multidentate N-containing ligands for the coordination to Group IV metal ions has resulted into original and quite unexpected coordinative architectures. Moving from proprietary amido-pyridinate ligands containing a “rolling” imidazole fragment featured by a classical “*mer*” coordination geometry around the metal ions, we have proposed the spatial redistribution of their donor atom set with the aim at preparing “scorpionate-like” systems suitable for an exclusive “*fac*” coordination to the metal center. At odds with our

expectations, the coordination behavior of the newly prepared chiral (racemic) ligands towards Group IV metal ions ($M^{IV} = \text{Zr, Hf}$) has led to unexpected assemblies. The benzyl-N-protected imidazole ligand ($L2^{Bn}$) gave discrete monometallic tris(dimethylamido) compounds of general formula $L2^{Bn}M(\text{NMe}_2)_3$. The ligand played as a monoanionic bidentate system $\kappa^2\{\text{N}^-, \text{N}\}$ for the metal ions, leaving behind an uncoordinated picolyl dangling arm. On the contrary, the unprotected $L2^H$ produced unique tetrameric assemblies named “poker complexes” due to the presence of regularly alternating (R^*, S^*, R^*, S^*) ligand enantiomers. Notably, the thermodynamically favored bis(dimethylamido) tetramers of Zr^{IV} and Hf^{IV} contain the imidazole fragment of each ligand bridging two neighboring M^{IV} ions [$\mu\text{-}\kappa\{\text{N}\}:\kappa\{\text{N}^-\}$] and the picolyl fragment “stinging” a neighboring metal center as an unconventional scorpion’s tail. The intrinsic ligands chirality (stemming from the presence of a stereogenic center in the ligand structure) is not resolved within their metal complexes because of the generation of *achiral* structures. New N-donor spatial arrangements are currently being scrutinized in our labs, to obtain new chiral ligands and related Group IV metal complexes.

Experimental Section

Materials and Methods. All reactions were performed using standard Schlenk procedures under a dry nitrogen or argon atmosphere. All the commercially available starting materials were of analytical grade. They were purchased from Aldrich or Stream Chemicals Inc. and used as received, without any further purification. Compounds **2**,^[40] **3**^[41] and 2-chloromethylpyridine^[42] (Scheme 3) were prepared according to literature procedures. Solvents were purified by standard distillation techniques. C_6D_6 , and CD_2Cl_2 (Aldrich) were stored over 4 Å molecular sieves and degassed by three freeze-pump-thaw cycles before use. NMR spectra were recorded on Bruker AVANCE 400 and 300 FT-NMR spectrometers. ^1H and $^{13}\text{C}\{^1\text{H}\}$ chemical shifts are reported in parts per million (ppm) downfield of tetramethylsilane (TMS)

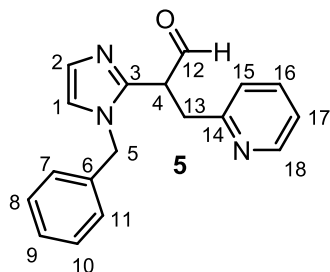
and were calibrated against the residual resonance of the deuterated solvent. Single crystal X-Ray data were collected at low temperature (100 or 120 K) on an Oxford Diffraction XCALIBUR 3 diffractometer equipped with a CCD area detector using Mo K α radiation (**8**, $\lambda = 0.7107 \text{ \AA}$) or a Cu K α radiation (**7**; $\lambda = 1.5418 \text{ \AA}$). The program used for the data collection was CrysAlis CCD 1.171^[66] Data reduction was carried out with the program CrysAlis RED 1.171^[67] and the absorption correction was applied with the program ABSPACK 1.17. Direct methods implemented in Sir97^[68] were used to solve the structures and the refinements were performed by full-matrix least-squares against F² implemented in SHELXL-2018.^[69] All the non-hydrogen atoms were refined anisotropically while the hydrogen atoms were fixed in calculated positions and refined isotropically with the thermal factor depending on the one of the atom to which they are bound. The geometrical calculations were performed by PARST97^[70] and molecular plots were produced by the program ORTEP3.^[71] CCDC-1939392 (**7**) and CCDC-1939393 (**8**) contain the supplementary crystallographic data for this paper.



Synthesis of 4. NaH (1.05 eq., 10.7 mmol) was added at 273 K to a solution of ethyl 2-(1-benzyl-1H-imidazol-2-yl)acetate (**3**) (2.50 g, 10.2 mmol) in dry and degassed DMF (50 mL). The mixture was stirred for 30 min at 273 K, then a solution of 2-(chloromethyl)pyridine (1.3 eq., 13.3 mmol) in dry and degassed DMF (10 mL) was added using a cannula needle. The resultant

mixture was stirred at room temperature for 2 h. Afterward, a saturated solution of NaHCO₃ (15 mL) was added. The organic product was extracted with AcOEt (15 mL) and the aqueous phase was washed with AcOEt (3 x 15 mL). The combined organic extracts were dried over Na₂SO₄ and, after removal of the solvent under reduced pressure, the residue was purified by silica gel flash chromatography (AcOEt) to give the product as yellow crystals (2.16 g, yield 63.2%).

^1H NMR (300 MHz, CDCl_3 , 293K): δ 1.08 (t, $^3J_{\text{HH}} = 7.1$ Hz, 3H, CH_2CH_3 , H^{14}), 3.54 (dd, $^3J_{\text{HH}} = 8.4$ Hz, $^2J_{\text{HH}} = 14.5$ Hz, 1H, H^{15}), 3.68 (dd, $^3J_{\text{HH}} = 6.8$ Hz, $^2J_{\text{HH}} = 14.5$ Hz, 1H, H^{15}), 4.10-3.93 (m, 2H, CH_2CH_3 , H^{13}), 4.55 (dd, $^3J_{\text{HH}} = 6.8$ Hz, $^3J_{\text{HH}} = 8.4$ Hz, 1H, CH , H^4), 5.09 (br s, 2H, CH_2Ph , H^5), 6.70 (br s, 1H, CH Imid, H^1), 7.05-6.94 (4H, CH Ar and CH Imid, $\text{H}^{2,8,10,19}$), 7.12 (m, 1H, CH Ar, H^{17}), 7.27-7.21 (3H, CH Ar, $\text{H}^{7,9,11}$), 7.47 (m, 1H, CH Ar, H^{18}), 8.39 (m, 1H, CH Ar, H^{20}). $^{13}\text{C}\{^1\text{H}\}$ NMR (75 MHz, CDCl_3 , 293 K): δ 13.9 (C^{14}), 38.4 (C^{15}), 42.5 (C^4), 49.3 (C^5), 61.2 (C^{13}), 120.1 (C^1), 121.3 (C^{19}), 124.1 (C^{17}), 126.9 ($\text{C}^{8,10}$), 127.8 (C^9), 128.1 (C^2), 128.7 ($\text{C}^{11,7}$), 136.1 (C^{18}), 136.2 (C^6), 144.6 (C^3), 149.0 (C^{20}), 158.4 (C^{16}), 170.5 (C^{12}).



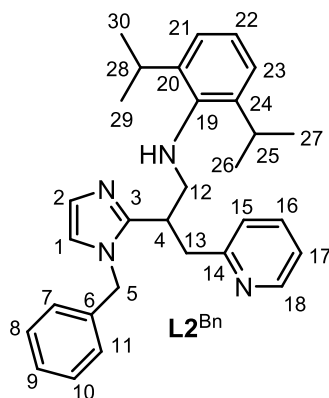
Synthesis of 5. DIBAL-H (1 M in toluene, 1.2 eq., 3.36 mL, 3.36 mmol) was

added dropwise to a solution of **4** (0.95 g, 2.83 mmol) in dry and degassed CH_2Cl_2 (15 mL) at 195 K under N_2 . The reaction was stirred for 0.5 h at that temperature before adding other 0.5 eq. of DIBAL-H. The resulting mixture was maintained under stirring at 195 K for other 0.5 h and then the reaction

was quenched with MeOH (5 mL). The mixture was allowed to warm up to room temperature and a saturated solution of potassium sodium tartrate was added to the mixture and stirred vigorously for an hour. The organic layer was separated, and the aqueous layer was extracted with CH_2Cl_2 (3 x 15 mL). The combined organic extracts were dried over Na_2SO_4 and, after removal of the solvent under reduced pressure, the residue was purified by silica gel flash chromatography (AcOEt : MeOH = 90 : 10) to give the product as a pale yellow oil (0.64 g, yield 78.0%).

^1H NMR (300 MHz, CD_2Cl_2 , 293K): δ 3.34 (dd, $^3J_{\text{HH}} = 7.8$ Hz, $^2J_{\text{HH}} = 14.8$ Hz, 1H, H^{13}), 3.67 (dd, $^3J_{\text{HH}} = 6.5$ Hz, $^2J_{\text{HH}} = 14.8$ Hz, 1H, H^{13}), 4.46 (m, 1H, H^4), 5.09 (br s, 2H, CH_2Ph , H^5), 6.90 (s, 1H, CH Imid, H^1), 7.15-7.05 (5H, CH Ar and CH Imid, $\text{H}^{2,8,10,15,17}$), 7.34-7.28 (3H, CH Ar, $\text{H}^{7,9,11}$), 7.57 (m, 1H, CH Ar, H^{16}), 8.48 (m, 1H, CH Ar, H^{18}), 9.63 (s, 1H, CHO , H^{12}). $^{13}\text{C}\{^1\text{H}\}$ NMR (75 MHz, CDCl_3 , 293 K): δ

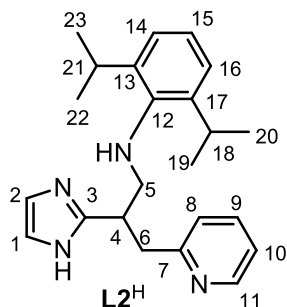
36.6 (C¹³), 49.3 (C^{4,5}), 120.8 (C¹), 121.5 (C¹⁷), 123.7 (C¹⁵), 126.9 (C^{8,10}), 127.9 (C⁹), 128.3 (C²), 128.8 (C^{7,11}), 136.2 (C¹⁶), 136.6 (C⁶), 143.6 (C³), 149.0 (C¹⁸), 158.2 (C¹⁴), 197.4 (C¹²).



Synthesis of L2^{Bn}. In a dry Schlenk tube, 2,6-diisopropylaniline (2.95 mL, 15.77 mmol, 5 eq.) was added to **5** (0.92 g, 3.15 mmol) and the mixture was heated at 373 K without stirring. The reaction was allowed to return to room temperature, the crude product was recovered with CH₂Cl₂, the solvent was evaporated under reduced pressure and the excess of 2,6-diisopropylaniline was removed with Kugelrohr. Afterwards, NaBH₃CN (0.30 g, 4.72 mmol)

and acetic acid (0.290 mL, 4.72 mmol) were added in sequence to a solution of the crude imine product in dry and degassed MeOH (10 mL) and THF (10 mL) and the resulting mixture was maintained under stirring and inert atmosphere at 323 K for 3 h. The reaction was quenched with a saturated solution of Na₂CO₃ (10 mL), the organic phase was separated and the aqueous layer was extracted with AcOEt (3 x 10 mL). The collected organic layers were dried over Na₂SO₄ and the solvent was evaporated under reduced pressure. The crude product was purified by flash chromatography (silica gel, petroleum ether : AcOEt = 30 : 70) to give **L2^{Bn}** as a pale yellow oil (1.07 g, yield 75%).

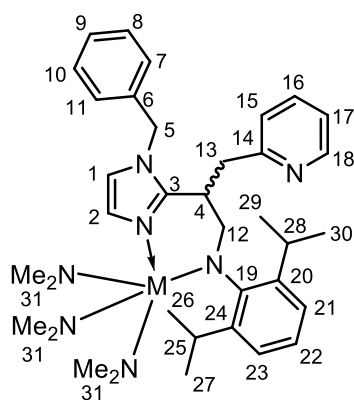
¹H NMR (300 MHz, CD₂Cl₂, 293K): δ 1.05 (d, ³J_{HH} = 6.8 Hz, 6H, H^{27,30}), 1.12 (d, ³J_{HH} = 6.8 Hz, 6H, H^{26,29}), 2.88 (dd, ³J_{HH} = 4.0 Hz, ²J_{HH} = 11.3 Hz, 1H, H^{12a}), 3.04 (sept, ³J_{HH} = 6.8 Hz, 2H, H^{25,28}), 3.29-3.22 (3H, H^{12b,13}), 3.84 (m, 1H, H⁴), 5.03 (br s, 2H, CH₂Ph, H⁵), 6.80 (br s, 1H, CH Imid, H¹), 7.12-6.97 (8H, CH Ar and CH Imid, H^{2,8,10,15,17,21,22,23}), 7.28-7.26 (3H, CH Ar, H^{7,9,11}), 7.53 (m, 1H, CH Ar, H¹⁶), 8.50 (m, 1H, CH Ar, H¹⁸). ¹³C{¹H} NMR (75 MHz, CD₂Cl₂, 293 K): δ 23.8 (C^{26,29}), 23.9 (C^{29,30}), 27.2 (C^{25,28}), 37.5 (C⁴), 40.8 (C¹³), 49.0 (C⁵), 54.4 (C¹²), 119.4 (C¹), 121.2 (C¹⁷), 123.2 (C^{21,23}), 123.5 (C²²), 123.8 (C¹⁵), 126.9 (C^{8,10}), 127.6 (C⁹), 127.7 (C²), 128.7 (C^{7,11}), 136.0 (C¹⁶), 137.0 (C⁶), 143.0 (C^{20,24}), 143.6 (C¹⁹), 149.2 (C¹⁸), 149.5 (C³), 159.7 (C¹⁴).



Synthesis of L2^H. A 100 mL stainless steel reactor, equipped with a magnetic stir bar, was charged, in a dry-box filled with nitrogen, with **6** (0.70 g, 1.54 mmol), 30 mL of dry and degassed MeOH and Pd(OH)₂/C 20 wt. % (Pearlman's catalyst, 0.350 g). The reactor was closed and filled with H₂ (3 bar). The final mixture was stirred at 323 K for 20 h. Afterwards the reactor was opened, the

mixture was recovered in a flask and the solvent was evaporated under reduced pressure. 20 mL of AcOEt were added and the suspension was passed through a Celite® pad. The solvent was removed and the crude product was purified by flash chromatography (silica gel, petroleum ether : AcOEt = 20 : 80, 5 % of NEt₃) to give L2^H as a white solid (0.25 g, yield 45%).

¹H NMR (400 MHz, CD₂Cl₂, 293K): δ 1.09 (d, ³J_{HH} = 6.9 Hz, 6H, H^{20,23}), 1.11 (d, ³J_{HH} = 6.9 Hz, 6H, H^{19,22}), 3.13-3.01 (4H, H^{5,18,21}), 3.26 (dd, ³J_{HH} = 6.0 Hz, ²J_{HH} = 14.4 Hz, 1H, H⁶), 3.36 (dd, ³J_{HH} = 7.5 Hz, ²J_{HH} = 14.4 Hz, 1H, H⁵), 3.73 (m, 1H, H⁴), 7.03-6.98 (5H, CH Ar and CH Imid, H^{1,2,14,15,16}), 7.18-7.15 (2H, CH Ar, H^{8,10}), 7.61 (m, 1H, CH Ar, H⁹), 8.54 (m, 1H, CH Ar, H¹¹). ¹³C{¹H} NMR (100 MHz, CD₂Cl₂, 293 K): δ 24.3 (C^{19,20,22,23}), 27.6 (C^{18,21}), 39.9 (C⁴), 40.3 (C⁶), 54.9 (C⁵), 121.9 (C¹⁰), 123.7 (C^{14,15,16}), 124.0 (C^{1,2}), 124.7 (C⁸), 137.1 (C⁹), 143.3 (C^{13,17}), 143.8 (C¹²), 149.2 (C¹¹), 150.4 (C³), 159.9 (C⁷).



M = Zr (**6**), Hf (**7**)

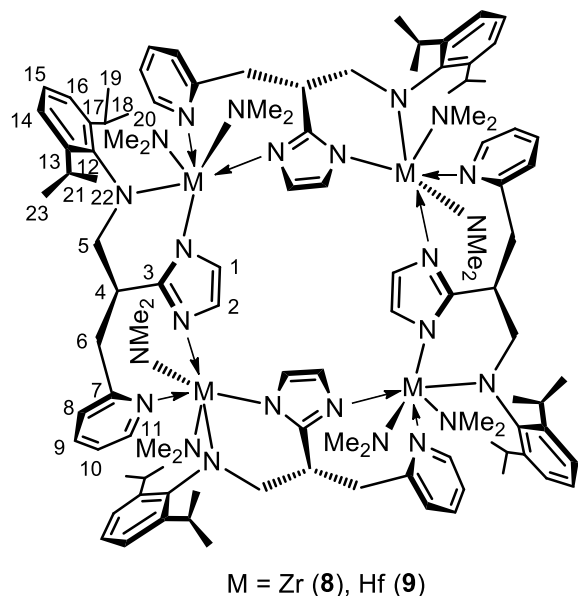
General procedure for the synthesis of complexes L2^{Bn}M^{IV}(NMe₂)₃ (M^{IV} = Zr, Hf) **6 and **7**.** A solution of L2^{Bn} (0.10 g, 0.22 mmol) in dry and degassed benzene (2 mL) was added dropwise to a solution of the proper metal precursor [M^{IV}(NMe₂)₄; M = Zr, Hf; 0.23 mmol, 1.05 eq.] in dry and degassed benzene (3 mL). The reaction mixture was maintained under stirring at room temperature for 30 min and then concentrated *in vacuo* to afford semisolid pale-yellow crude materials that were washed with cold

n-pentane and dried in vacuo to give **L2^{Bn}Zr^{IV}(NMe₂)₃** (**6**) and **L2^{Bn}Hf^{IV}(NMe₂)₃** (**7**) as white solids. Crystals of **7** suitable for X-ray diffraction analysis were grown from concentrated *n*-pentane solution cooled at 243 K.

6: (91% yield of the isolated product); ¹H NMR (400 MHz, C₆D₆, 293K): δ 1.22 (d, ³J_{HH} = 6.8 Hz, 3H, H²⁷), 1.29 (d, ³J_{HH} = 6.8 Hz, 3H, H³⁰), 1.47 (d, ³J_{HH} = 6.8 Hz, 3H, H²⁶), 1.56 (d, ³J_{HH} = 6.8 Hz, 3H, H²⁹), 3.07 (br s, 18H, N(CH₃)₂, H³¹), 3.49-3.34 (3H, H^{12b,13}), 3.65 (sept, ³J_{HH} = 6.8 Hz, 1H, H²⁵), 3.78 (m, 1H, H⁴), 4.10-4.02 (2H, H^{12a,28}), 4.32 (d, ABq, ²J_{HH} = 15.7 Hz, 1H, CHHPh, H^{5b}), 4.59 (d, ABq, ²J_{HH} = 15.7 Hz, 1H, CHHPh, H^{5a}), 6.14 (d, ³J_{HH} = 1.5 Hz, 1H, CH Imid, H¹), 6.52-6.48 (2H, CH Ar, H^{15,17}), 6.74-6.72 (m, 2H, CH Ar, H^{7,11}), 6.84 (m, 1H, CH Ar, H¹⁶), 6.92 (d, ³J_{HH} = 1.5 Hz, 1H, CH Imid, H²), 6.98-6.94 (3H, CH Ar, H^{8,9,10}), 7.00 (m, CH Ar, 1H, H²²), 7.24-7.08 (2H, CH Ar, H^{21,23}), 8.32 (m, CH Ar, 1H, H¹⁸). ¹³C{¹H} NMR (100 MHz, C₆D₆, 293 K): δ 24.2 (C²⁹), 24.5 (C²⁶), 27.1 (C³⁰), 27.4 (C²⁷), 28.5 (C²⁸), 28.5 (C²⁵), 39.6 (C⁴), 40.8 (C¹³), 44.0 (C³¹), 49.3 (C⁵), 61.1 (C¹²), 119.4 (C¹), 121.4 (C¹⁷), 123.6 (C¹⁵), 123.7 (C²¹), 123.8 (C²³), 123.9 (C²²), 127.1 (C^{7,11}), 127.9 (C^{2,9}), 129.0 (C^{8,10}), 136.0 (C¹⁶), 136.2 (C⁶), 145.4 (C²⁴), 145.6 (C²⁰), 149.5 (C¹⁸), 152.0 (C¹⁹), 153.3 (C³), 160.1 (C¹⁴).

7: (87% yield of the isolated product); ¹H NMR (400 MHz, C₆D₆, 293K): δ 1.21 (d, ³J_{HH} = 6.8 Hz, 3H, H²⁷), 1.28 (d, ³J_{HH} = 6.8 Hz, 3H, H³⁰), 1.47 (d, ³J_{HH} = 6.8 Hz, 3H, H²⁶), 1.57 (d, ³J_{HH} = 6.8 Hz, 3H, H²⁹), 3.10 (br s, 18H, N(CH₃)₂, H³¹), 3.48-3.42 (m, 2H, H¹³), 3.69-3.58 (2H, H^{12b,25}), 3.77 (m, 1H, H⁴), 4.11-4.07 (2H, H^{12a,28}), 4.32 (d, ABq, ²J_{HH} = 15.7 Hz, 1H, CHHPh, H^{5b}), 4.57 (d, ABq, ²J_{HH} = 15.7 Hz, 1H, CHHPh, H^{5a}), 6.13 (d, ³J_{HH} = 1.5 Hz, 1H, CH Imid, H¹), 6.51-6.48 (2H, CH Ar, H^{15,17}), 6.73-6.71 (m, 2H, CH Ar, H^{7,11}), 6.84 (m, 1H, CH Ar, H¹⁶), 6.98-6.94 (4H, CH Ar and CH Imid, H^{2,8,9,10}), 7.10 (m, 1H, CH Ar, H²²), 7.25-7.18 (2H, CH Ar, H^{21,23}), 8.30 (m, 1H, CH Ar, H¹⁸). ¹³C{¹H} NMR (100 MHz, C₆D₆, 293 K): δ 24.2 (C²⁹), 24.5 (C²⁶), 27.3 (C³⁰), 27.6 (C²⁷), 28.4 (C²⁸), 28.7 (C²⁵), 39.6 (C⁴), 40.6 (C¹³), 43.9 (C³¹), 49.3 (C⁵), 61.3 (C¹²), 119.7 (C¹), 121.4 (C¹⁷), 123.7 (C¹⁵), 123.8 (C^{21,22,23}), 127.1 (C^{7,11}), 127.0

(C^{2,9}), 129.0 (C^{8,10}), 136.0 (C¹⁶), 136.1 (C⁶), 145.6 (C²⁴), 145.6 (C²⁰), 149.5 (C¹⁸), 152.1 (C¹⁹), 153.5 (C³), 159.9 (C¹⁴).



General procedure for the synthesis of complexes **8** and **9**.

A solution of **L2^H** (0.15 g, 0.41 mmol) in dry and degassed aromatic solvent (4 mL; benzene for **8** and toluene for **9**) was treated dropwise with a solution of the proper metal precursor ($[M^{IV}(NMe_2)_4]$ 99%; M=Zr, Hf; 1.05 equiv.) in dry and degassed aromatic solvent (4 mL; benzene for **8** and toluene for **9**). The reaction mixture was stirred at desired temperature (343 K for **8** and 373 K for **9**) for the appropriate reaction time (7 h for **8** and 15 h for

9) and then it was concentrated in *vacuo* to afford a yellow solid. The product was purified by crystallization from hot *n*-pentane by cooling the resulting solution at r.t overnight to afford **8** and **9** as pale yellow micro-crystals. Suitable crystals of **8** for X-ray diffraction were collected after successive recrystallization from hot *n*-pentane.

8: (61% yield of the isolated product); ¹H NMR (400 MHz, C₆D₆, 293K): δ 0.87 (d, ³J_{HH} = 6.7 Hz, 3H, H²⁰), 1.14 (d, ³J_{HH} = 6.7 Hz, 3H, H¹⁹), 1.56 (d, ³J_{HH} = 6.7 Hz, 3H, H²³), 1.64 (d, ³J_{HH} = 6.7 Hz, 3H, H²²), 2.87-2.59 (13H, NMe₂, H^{6a}), 3.21 (m, 1H, H^{5a}), 3.60-3.46 (2H, H^{5b,18}), 4.48 (m, 1H, H⁴), 4.84-4.48 (2H, H^{6b,21}), 5.36 (s, 1H, H²), 5.90 (s, 1H, H¹), 6.36 (m, 1H, H⁸), 6.78-6.67 (2H, H^{9,10}), 7.28-7.19 (2H, H^{14,15}), 7.47 (m, 1H, H¹⁶), 8.12 (m, 1H, H¹¹). ¹³C{¹H} NMR (100 MHz, C₆D₆, 293 K): δ 23.4 (C²²), 23.8 (C¹⁹), 27.2 (C¹⁸), 27.3 (C²¹), 27.5 (C²³), 27.8 (C²⁰), 37.9 (C⁶), 41.8 (C⁴), 45.3 (C, NMe₂), 46.2 (C, NMe₂), 67.5 (C⁵), 120.4 (C¹⁰), 123.1 (C¹⁶), 123.2 (C¹⁴), 123.4 (C¹⁵), 124.8 (C¹), 126.2 (C⁸), (C² overlaps with C₆D₆), 136.9 (C⁹), 144.2 (C¹⁷), 144.5 (C¹³), 151.4 (C¹¹), 155.5 (C¹²), 155.7 (C³), 159.0 (C⁷).

9: (58% yield of the isolated product); ^1H NMR (400 MHz, C_6D_6 , 293K): δ 0.90 (d, $^3J_{\text{HH}} = 6.8$ Hz, 3H, H^{20}), 1.15 (d, $^3J_{\text{HH}} = 6.8$ Hz, 3H, H^{19}), 1.55 (d, $^3J_{\text{HH}} = 6.8$ Hz, 3H, H^{23}), 1.64 (d, $^3J_{\text{HH}} = 6.8$ Hz, 3H, H^{22}), 3.05-2.33 (13H, NMe_2 , H^{6a}), 3.37 (m, 1H, H^{5a}), 3.53 (sept, $^3J_{\text{HH}} = 6.8$ Hz, 1H, H^{18}), 3.67 (m, 1H, H^{5b}), 4.46 (m, 1H, H^4), 4.90-4.77 (2H, $\text{H}^{6b,21}$), 5.36 (s, 1H, H^2), 5.86 (s, 1H, H^1), 6.35 (m, 1H, H^8), 6.79-6.70 (2H, $\text{H}^{9,10}$), 7.20 (m, 1H, H^{15}), 7.29 (m, 1H, H^{14}), 7.49 (m, 1H, H^{16}), 8.17 (m, 1H, H^{11}). $^{13}\text{C}\{^1\text{H}\}$ NMR (100 MHz, C_6D_6 , 293 K): δ 23.3 (C^{22}), 23.9 (C^{19}), 27.4 (C^{18}), 27.6 (C^{21}), 27.8 (C^{23}), 28.1 (C^{20}), 37.6 (C^6), 42.2 (C^4), 45.4 (C, NMe_2), 46.3 (C, NMe_2), 67.1 (C^5), 120.9 (C^{10}), 123.4 (C^{16}), 123.6 (C^{14}), 123.7 (C^{15}), 125.5 (C^1), 126.6 (C^8), (C^2 overlaps with C_6D_6), 137.2 (C^9), 145.0 (C^{17}), 145.4 (C^{13}), 152.0 (C^{11}), 155.7 (C^{12}), 156.9 (C^3), 159.5 (C^7).

Supporting Information (see footnote on the first page of this article): ^1H and $^{13}\text{C}\{^1\text{H}\}$ NMR spectra of reaction intermediates **4** and **5**, of the ligands $\text{L}2^{\text{Bn}}$ and $\text{L}2^{\text{H}}$, of complexes **6**, **7**, **8** and **9**. Collective table containing the main crystallographic data, experimental details and structure refinement details for **7** and **8**. ORTEP representation of the X-ray structure of the $\mu\text{-}\kappa^2\{\text{N}^-, \text{N}^-\}:\kappa^2\{\text{N}, \text{N}\}$ tetrameric complex **8** with the assigned atom labels.

Acknowledgments

G.T. and G.G. thank the Italian MIUR through the PRIN 2015 Project SMARTNESS (2015K7FZLH) for financial support. G.G. thanks the TRAINER project (Catalysts for Transition to Renewable Energy Future) Ref. ANR-17-MPGA-0017 for support. A.R., L.L. and G.G. would like to acknowledge the bilateral project CNR (Italy) – RFBR (Russian Federation) 2018-2020 for financial support.

References

- [1] D. Janssen-Muller, C. Schleppehorst, F. Glorius, *Chem. Soc. Rev.* **2017**, *46*, 4845-4854.
- [2] R. Arévalo, M. Espinal Viguri, M. A. Huertos, J. Pérez, L. Riera, *Adv. Organomet. Chem.* **2016**, *65*, 47-114.
- [3] W.-H. Wang, J. T. Muckerman, E. Fujita, Y. Himeda, *New J. Chem.* **2013**, *37*, 1860-1866.
- [4] J. A. Mata, M. Poyatos, P. Peris, *Coord. Chem. Rev.* **2007**, *251*, 841-859.
- [5] L. Cavallo, A. Correa, C. Costabile, H. Jacobsen, *J. Organomet. Chem.* **2005**, *690*, 5407-5413.
- [6] A. A. Danopoulos, T. Simler, P. Braunstein, *Chem. Rev.* **2019**, *119*, 3730-3961.
- [7] M.-M. Gan, J.-Q. Liu, L. Zhang, Y.-Y. Wang, F. Ekkehardt Hahn, Y.-F. Han, *Chem. Rev.* **2018**, *118*, 9587-9641.
- [8] L. M. T. Frija, A. J. L. Pombeiro, M. N. Kopylovich, *Eur. J. Org. Chem.* **2017**, 2670-2682.
- [9] A. Adach, *J. Coord. Chem.* **2017**, *70*, 757-779.
- [10] X. Wang, A. Tian, X. Wang, *RSC Adv.* **2015**, *5*, 41155-41168.
- [11] P. I. P. Elliott, *Organomet. Chem.* **2014**, *39*, 1-25.
- [12] S. Bellemin-Laponnaz, S. Dagorne, *Chem. Rev.* **2014**, *114*, 8747-8774.
- [13] D. Pugh, A. A. Danopoulos, *Coord. Chem. Rev.* **2007**, *251*, 610-641.
- [14] F. Dumur, E. Dumas, C. R. Mayer, in *Targets in Heterocyclic Systems; Chemistry and Properties*, Vol. 11, Italian Society of Chemistry, **2007**, pp. 70-103.
- [15] P. A. Scattergood, A. Sinopoli, P. I. P. Elliott, *Coord. Chem. Rev.* **2017**, *350*, 136-154.
- [16] C. Pettinari, R. Pettinari, C. Di Nicola, F. Marchetti, in *Advances in Organometallic Chemistry and Catalysis* (Ed.: A. J. L. Pombeiro), John Wiley & Sons, Inc., **2014**, pp. 269-284.
- [17] R. Mukherjee, *Coord. Chem. Rev.* **2000**, *203*, 151-218.
- [18] S. Friedrich, M. Schubart, L. H. Gade, I. J. Scowen, A. J. Edwards, M. McPartlin, *Chem. Ber.* **1997**, *130*, 1751-1759.

- [19] P. Mehrkhodavandi, R. R. Schrock, P. J. J. Bonitatebus, *Organometallics* **2002**, *21*, 5785-5798.
- [20] P. Mehrkhodavandi, P. J. J. Bonitatebus, R. R. Schrock, *J. Am. Chem. Soc.* **2000**, *122*, 7841-7842.
- [21] R. R. Schrock, J. Adamchuk, K. Ruhland, L. P. H. Lopez, *Organometallics* **2003**, *22*, 5079-5091.
- [22] N. Vujkovic, B. D. Ward, A. Maisse-Francois, H. Wadepohl, P. Mountford, L. H. Gade, *Organometallics* **2007**, *26*, 5522-5534.
- [23] T. Gehrman, J. L. Fillol, S. A. Scholl, H. Wadepohl, L. H. Gade, *Angew. Chem. Int. Ed.* **2011**, *50*, 5757-5761.
- [24] T. Gehrman, S. A. Scholl, J. L. Fillol, H. Wadepohl, L. H. Gade, *Chem. Eur. J.* **2012**, *18*, 3925-3941.
- [25] S. A. Scholl, H. Wadepohl, L. H. Gade, *Organometallics* **2013**, *32*, 937-940.
- [26] L. Luconi, G. Giambastiani, A. Rossin, C. Bianchini, A. Lledos, *Inorg. Chem.* **2010**, *49*, 6811-6813.
- [27] L. Luconi, A. Rossin, G. Tuci, I. Tritto, L. Boggioni, J. J. Klosin, C. N. Theriault, G. Giambastiani, *Chem. Eur. J.* **2012**, *18*, 671-687.
- [28] L. Luconi, A. Rossin, A. Motta, G. Tuci, G. Giambastiani, *Chem. Eur. J.* **2013**, *19*, 4906-4921.
- [29] L. Luconi, J. Klosin, A. J. Smith, S. Germain, E. Schulz, J. Hannedouche, G. Giambastiani, *Dalton Trans.* **2013**, *42*, 16056-16065.
- [30] L. Luconi, A. Rossin, G. Tuci, S. Germain, E. Schulz, J. Hannedouche, G. Giambastiani, *ChemCatChem* **2013**, *5*, 1142-1151.
- [31] L. Luconi, A. A. Kissel, A. Rossin, N. M. Khamaletdinova, A. V. Cherkasov, G. Tuci, G. K. Fukin, A. A. Trifonov, G. Giambastiani, *New J. Chem.* **2017**, *41*, 540-551.
- [32] L. Luconi, A. Rossin, G. Tuci, Z. Gafurov, D. M. Lyubov, A. A. Trifonov, S. Cicchi, H. Ba, C. Pham-Huu, D. Yakhvarov, G. Giambastiani, *ChemCatChem* **2019**, *11*, 495-510.

- [33] D. M. Lyubov, G. K. Fukin, A. V. Cherkasov, A. S. Shavyrin, A. A. Trifonov, L. Luconi, C. Bianchini, A. Meli, G. Giambastiani, *Organometallics* **2009**, *28*, 1227-1232.
- [34] L. Luconi, D. M. Lyubov, C. Bianchini, A. Rossin, C. Faggi, G. K. Fukin, A. V. Cherkasov, A. S. Shavyrin, A. A. Trifonov, G. Giambastiani, *Eur. J. Inorg. Chem.* **2010**, 608-620.
- [35] A. A. Karpov, A. V. Cherkasov, G. K. Fukin, A. S. Shavyrin, L. Luconi, G. Giambastiani, A. A. Trifonov, *Organometallics* **2013**, *32*, 2379-2388.
- [36] D. M. Lyubov, L. Luconi, A. Rossin, G. Tuci, A. V. Cherkasov, G. K. Fukin, G. Giambastiani, A. A. Trifonov, *Chem. Eur. J.* **2014**, *20*, 3487-3499.
- [37] L. Luconi, D. M. Lyubov, A. Rossin, T. A. Glukhova, A. V. Cherkasov, G. Tuci, G. K. Fukin, A. A. Trifonov, G. Giambastiani, *Organometallics* **2014**, *33*, 7125-7134.
- [38] S.-S. Chen, *Crystengcomm* **2016**, *18*, 6543-6565.
- [39] P. Sander, I. Geibel, C. Witte, S. Hüller, M. Schmidtman, R. Beckhaus, *Eur. J. Inorg. Chem.* **2018**, 3717-3724.
- [40] A. A. Macco, E. F. Godefroi, J. J. M. Drouen, *J. Org. Chem.* **1975**, *2*, 252-255.
- [41] D. Ray, J. T. Foy, R. P. Hughes, I. Aprahamian, *Nat. Chem.* **2012**, *4*, 757-762.
- [42] P. Herold, S. Stutz, R. Mah, V. Tschinke, A. Stojanovic, N. Jotterand, M. Quirnbach, D. Behnke, C. Marti WO/2005/090304, **2005**.
- [43] M. A. H. Moelands, D. J. Schamhart, E. Folkertsma, M. Lutz, A. L. Spek, R. J. M. K. Gebbink, *Dalton Trans.* **2014**, *43*, 6769-6785.
- [44] X.-m. Gan, I. Binyamin, B. M. Rapko, J. Fox, E. N. Duesler, R. T. Paine, *Inorg. Chem.* **2004**, *43*, 2443-2448.
- [45] C. Bianchini, G. Giambastiani, I. Guerrero Rios, A. Meli, W. Oberhauser, A. M. Segarra, L. Sorace, A. Toti, *Organometallics* **2007**, *26*, 4639-4651.

- [46] C. Bianchini, G. Giambastiani, I. Guerrero Rios, A. Meli, W. Oberhauser, L. Sorace, A. Toti, *Organometallics* **2007**, *26*, 5066-5078.
- [47] M. M. Salter, J. Kobayashi, Y. Shimizu, S. Kobayashi, *Org. Lett.* **2006**, *8*, 3533-3536.
- [48] M. E. Jung, Z. Longmei, P. Tangsheng, Z. Huiyan, L. Yan, S. Jingyu, *J. Org. Chem.* **1993**, *57*, 3528-3530.
- [49] S. W. Goldstein, L. E. Overman, M. H. Rabinowitz, *J. Org. Chem.* **1992**, *57*, 1179-1190.
- [50] P. A. Jacobi, M. J. Martinelli, S. Polanc, *J. Am. Chem. Soc.* **1984**, *106*, 5594-5598.
- [51] Z. Wang, in *Comprehensive Organic Name Reactions and Reagents*, John Wiley & Sons, Inc., **2010**, pp. 2143-2146.
- [52] M. Lautens, S. Kumanovic, C. Meyer, *Angew. Chem. Int. Ed.* **1996**, *35*, 1329-1330.
- [53] B. Wang, D. Chu WO2011130661A1, **2011**.
- [54] The calculated t index of trigonality for **7** is 0.86. For calculations of t values see: A. W. Addison, T. N. Rao, J. Reedijk, J. van Rijn, G. C. Verschoor, *J. Chem. Soc. Dalton Trans.* **1984**, 1349-1356.
- [55] G. M. Diamond, K. A. Hall, A. M. LaPointe, M. K. Leclerc, J. Longmire, J. A. W. Shoemaker, P. Sun, *ACS Catal.* **2011**, *1*, 887-900.
- [56] K. A. Frazier, R. D. Froese, Y. He, J. Klosin, C. N. Theriault, P. C. Vosejka, Z. Zhou, K. A. Abboud, *Organometallics* **2011**, *30*, 3318-3329.
- [57] R. D. J. Froese, B. A. Jazdzewski, J. Klosin, R. L. Kuhlman, C. N. Theriault, D. M. Welsh, K. A. Abboud, *Organometallics* **2011**, *30*, 251-262.
- [58] I. Haas, W. P. Kretschmer, R. Kempe, *Organometallics* **2011**, *30*, 4854-4861.
- [59] C. Zuccaccia, A. Macchioni, V. Busico, R. Cipullo, G. Talarico, F. Alfano, H. W. Boone, K. A. Frazier, P. D. Hustad, J. C. Stevens, P. C. Vosejka, K. A. Abboud, *J. Am. Chem. Soc.* **2008**, *130*, 10354-10368.

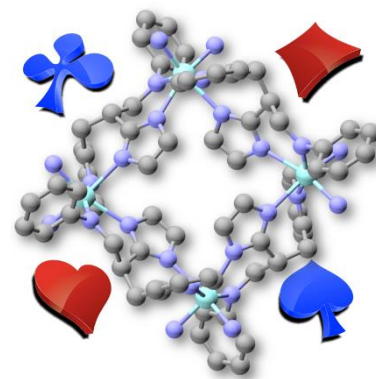
- [60] D. Rottger, G. Erker, R. Frohlich, S. Kotila, *J. Organomet. Chem.* **1996**, *518*, 17-19.
- [61] S. Aharonovich, M. Botoshansky, R. M. Waymouth, M. S. Eisen, *Inorg. Chem.* **2010**, *49*, 9217-9229.
- [62] M. Farina, C. Morandi, *Tetrahedron* **1974**, *30*, 1819-1831.
- [63] G. E. Mc Casland, S. Proskow, *J. Am. Chem. Soc.* **1955**, *77*, 4687-4688.
- [64] G. E. Mc Casland, S. Proskow, *J. Am. Chem. Soc.* **1956**, *78*, 5646-5652.
- [65] G. E. Mc Casland, R. Horvat, M. R. Roth, *J. Am. Chem. Soc.* **1959**, *81*, 2399-2402.
- [66] CrysAlisCCD 1.171.31.2 (release 07-07-2006); CrysAlis171.NET, Oxford Diffraction Ltd.
- [67] CrysAlis RED 1.171.31.2 (release 07-07-2006); CrysAlis171.NET, Oxford Diffraction Ltd.
- [68] A. Altomare, M. C. Burla, M. Camalli, G. L. Casciarano, C. Giacovazzo, A. Guagliardi, A. G. G. Moliterni, P. G., R. Spagna, *J. Appl. Crystallogr.* **1999**, *32*, 115-119.
- [69] G. M. Sheldrick, *Acta Cryst.* **2015**, *C71*, 3-8.
- [70] M. Nardelli, *Comput. Chem.* **1993**, *7*, 95-98.
- [71] L. J. Farrugia, *J. Appl. Crystallogr.* **1997**, *30*, 565.

TOC graphic

Key Topics: Zirconium(IV) – Hafnium(IV) – imidazole –
supramolecular assembly – N-ligands

TOC Text:

The unprotected imidazole-containing N₄-tetradentate ligand N-(2-(1H-imidazol-2-yl)-3-(pyridin-2-yl)propyl)-2,6-diisopropylaniline gives rise to a tetrameric “poker” complex in combination with Zr^{IV} and Hf^{IV} ions. Its benzyl-N-protected counterpart generates discrete monometallic coordination compounds instead. This simple ligand protection on the imidazole ring induces deep modifications of its coordination modes towards early transition metals.



Twitter Accounts: @GiulGiamba @RossinAndrea @StampaCnr